

## Structural studies of glassy $\text{CuAsSe}_2$ and $\text{Cu-As}_2\text{Se}_3$ alloys\*

K. S. Liang<sup>†</sup>

*Department of Applied Physics, Stanford University, Stanford, California 94305*

A. Bienenstock and C. W. Bates

*Materials Science and Engineering Department, Stanford University, Stanford, California 94305*

(Received 8 April 1974)

X-ray-diffraction radial-distribution, electron-spectroscopy-for-chemical-analysis (ESCA), crystallization, and differential-thermal-analysis (DTA) studies of glassy  $\text{Cu}_x(\text{As}_{0.4}\text{Se}_{0.6})_{100-x}$  alloys, with  $0 \leq x \leq 30$ , as well as  $\text{CuAsSe}_2$ , have been performed. The alloy radial-distribution-function (rdf) results indicate that the average nearest-neighbor coordination number increases from 2.4 for  $x = 0$  to 3.83 for  $x = 30$ . The  $\text{CuAsSe}_2$  rdf is similar to those of amorphous Ge and Si and indicates an average nearest-neighbor coordination number of a little less than 4, indicating that the atomic arrangement in the compound is similar to that in the amorphous elements. The rdf results, when coupled with the ESCA, DTA, and crystallization studies, imply that large regions of the  $\text{Cu-As}_2\text{Se}_3$  alloys have an atomic arrangement and composition close to that of glassy  $\text{CuAsSe}_2$ . These results are used to rationalize the marked decrease of the band gap, increase of the conductivity, and much of the observed  $T_g$  variation with increasing Cu concentration in the alloys. Also included in this paper is a derivation of a new random covalent model which corrects inconsistencies in that model which has been used frequently to analyze the structures of amorphous germanium-chalcogen alloys.

### I. INTRODUCTION

The conductivities of amorphous semiconductors are generally much less sensitive to nonstoichiometry and the presence of impurities than are those of crystalline semiconductors. The large conductivity increases caused by the additions of Cu,<sup>1,2</sup> Ag,<sup>2,3</sup> Ga,<sup>4</sup> In,<sup>4</sup> and Tl (Ref. 4) in  $\text{As}_2\text{Se}_3$ , as well as Cu and Ag in  $\text{As}_2\text{S}_3$  (Ref. 3 and 5) are, however, exceptions to this general rule.

The common insensitivity of amorphous-semiconductor conductivities has been explained by Mott,<sup>6</sup> who postulated that the impurities are coordinated in keeping with the  $8 - N$  rule such that their covalent bonding requirements are satisfied. As a result, they do not form donor or acceptor states and produce no large change in the conductivity. Structural verification of this model appears to have been supplied by structural studies of amorphous  $\text{Ge}_x\text{Te}_{1-x}$  alloys by Betts *et al.*<sup>7</sup> which indicate fourfold and twofold coordination of the Ge and Te, respectively, in keeping with Mott's picture. This result was unexpected since there is no crystalline compound in the binary system with such coordination. Similarly, structural studies by Renninger and Averbach,<sup>8</sup> as well as by Liang<sup>9</sup> on  $\text{As}_x\text{Se}_{1-x}$  support a model in which the As and Se are threefold and twofold coordinated, respectively, in keeping with the picture. These studies, when taken with others, tend to suggest that the picture is valid for many amorphous alloys formed of group-IV, -V, and -VI elements.

Mott's structural picture does not seem applicable to the exceptions discussed above because the

conductivity changes are large and because most of the impurity elements cited are not commonly found in coordinations associated with the  $8 - N$  rule. Since no structural work, to our knowledge, has been performed on them, we undertook this study of  $\text{Cu-As}_2\text{Se}_3$  alloys. In the course of this work it became apparent that it would also be valuable to perform structural studies of amorphous  $\text{CuAsSe}_2$ .

Before presenting these structural studies, we briefly review other types of studies on them.

The electrical properties of amorphous  $\text{Cu-As}_2\text{Se}_3$  alloys were first reported by Danilov and Myuller,<sup>1</sup> who showed that a 5-at. % addition of Cu to  $\text{As}_2\text{Se}_3$  leads to a conductivity increase of approximately four orders of magnitude. The thermal and optical energy gaps were also shown, by Danilov and Mosli<sup>2</sup> as well as Andreichin,<sup>10</sup> to decrease with increasing Cu content. This gap decrease could account for much of the conductivity increase.

Several possible causes of this type of energy-gap decrease have been postulated.<sup>9,11,12</sup> To explain the corresponding role of Ag in  $\text{As}_2\text{S}_3$ , Mott and Davis<sup>12</sup> assume the existence of a significant band tail of localized states into the energy gap. The decrease of the activation energy is then conjectured to be due to a decrease in the range of the localized states. That is, the valence-band mobility edge is assumed to move towards the band edge, leading to a decrease in the activation energy for electrical conduction. They suppose that the increased conductivity arises not from the formation of impurity levels, but from structural changes (caused by the presence of Ag) of such a kind as to

reduce the disorder. These authors do not discuss the nature of the structural change.

In this work, the nature of the structural change is examined in detail for some glasses in the Cu-As-Se system.  $\text{Cu}_x(\text{As}_{0.4}\text{Se}_{0.6})_{100-x}$  alloys, with  $0 \leq x \leq 30$ , as well as  $\text{CuAsSe}_2$  were studied with radial-distribution analysis, electron spectroscopy for chemical analysis (ESCA), crystallization analysis, and differential thermal analysis (DTA). On the basis of these studies, a tentative structural picture is put forth which rationalizes the band-gap decreases.

It is shown that glassy  $\text{CuAsSe}_2$  probably has a structure in which the atoms are tetrahedrally coordinated. It has a radial-distribution function (rdf) which is quite similar to those of amorphous Ge and Si. The high-Cu-concentration Cu-As $_2$ Se $_3$  glassy alloys probably also have large regions of tetrahedral coordination with a composition close to  $\text{CuAsSe}_2$ . These conclusions are supported by the ESCA, DTA, and crystallization studies.

In the course of the analysis, it became apparent that the random covalent model,<sup>7</sup> which has been used extensively to interpret germanium-chalcogen rdf's, has a conceptual inconsistency. A new version of this model is derived in the Appendix and analyzed in the text.

## II. SAMPLE PREPARATION

The syntheses of the amorphous samples were carried out in evacuated ( $10^{-6}$  torr) quartz ampoules with high- (99.9999%) purity elements as starting materials. The samples were heated in a rocking furnace at approximately 850 °C for about 24 h, and then water quenched. X-ray-diffraction studies were performed to assure that no crystalline phases were present. Glassy samples with  $x$  up to 30 could easily be obtained in this manner.

Recently, the glass-forming region of the Cu-As-Se system has been investigated by Savan *et al.*<sup>13</sup> and by Asahara and Izumitani,<sup>14</sup> who find maximum  $x$  values of 32.43 and 35, respectively.

## III. DTA AND X-RAY-DIFFRACTION STUDY

DTA experiments were carried out on a DuPont differential thermal analyzer, model 900. Crushed samples were sealed in 5-mm quartz ampoules at about  $5 \times 10^{-4}$  torr. The heating rate was 20 °C/min. The thermograms of alloys with  $x = 0, 5, 10, 20,$  and 30 are shown in Fig. 1.

The glass transition temperature  $T_g$ , which is indicated by the small endotherm near 200 °C, decreases with the addition of up to approximately 5-at. % Cu and then increases with increasing Cu concentration, as is shown in Fig. 2. The cause of the decrease at low concentrations has not been determined in this work. The subsequent increase is discussed after the structural work is presented.

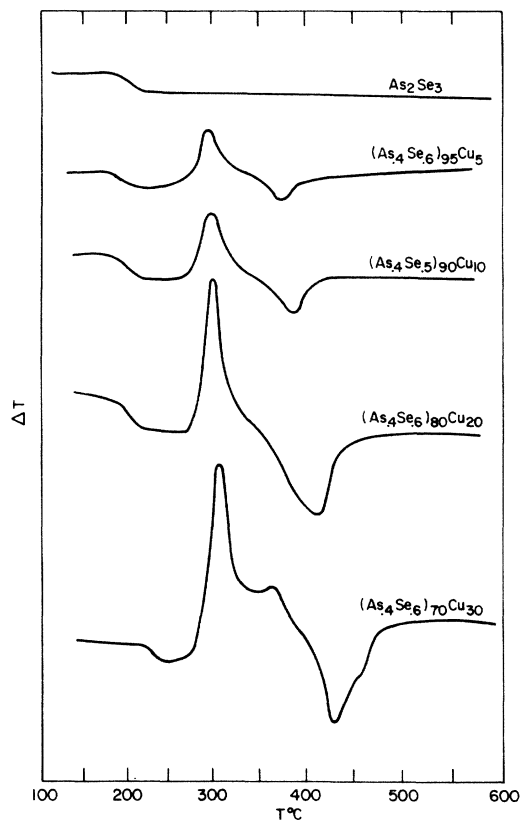


FIG. 1. DTA traces for amorphous Cu-As $_2$ Se $_3$  alloys.

As the temperature is increased above  $T_g$ , the pure As $_2$ Se $_3$  changes continuously into the liquid state. The samples containing Cu devitrify prior to melting, as is indicated by the exothermic peaks shown on the thermograms. In an effort to obtain hints of the atomic arrangements in the glasses, x-ray-diffraction patterns of the first crystallization products were obtained. The partial devitrification was achieved by heating the sample inside the DTA cell up to a temperature just above the exothermic peak and then cooling it. The diffraction patterns from such samples, taken with Cu K $\alpha$  radiation are shown in Fig. 3. These indicate that the crystalline phase so obtained has the sphalerite structure with a lattice constant of  $5.49 \pm 0.02$  Å.

In an effort to identify this phase, a literature survey of binary and ternary Cu-As-Se compounds was performed. No binary compounds could account for the diffraction pattern. Two ternary compounds, CuAsSe $_2$  (Ref. 15) and Cu $_3$ AsSe $_4$ ,<sup>16</sup> were found to have crystal structures close to sphalerite. Their diffraction patterns are shown in Fig. 4. (Crystalline CuAsSe $_2$  of stated 99.99% purity was purchased from Space Electronics Products, Inc. Crystalline Cu $_3$ AsSe $_4$  was prepared

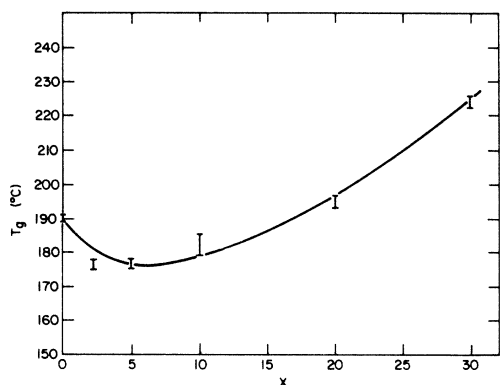


FIG. 2. Plot of glass transition temperature ( $T_g$ ) versus atomic percent of copper in amorphous  $\text{Cu}_x(\text{As}_{0.4}\text{Se}_{0.6})_{100-x}$  alloys.

by slow cooling of the melt.)

Both diffraction patterns are very similar to those obtained from the devitrified portions of the glasses, with almost-cubic  $d$  spacings and three intense low-angle peaks followed by a succession of weaker peaks. Both, however, show evidence of small distortions from the sphalerite structure. This is most evident in  $\text{Cu}_3\text{AsSe}_4$ , in which even the second- and third-lowest-angle peaks are split into well resolved doublets. The splitting is barely discernible in  $\text{CuAsSe}_2$ . It should also be noted

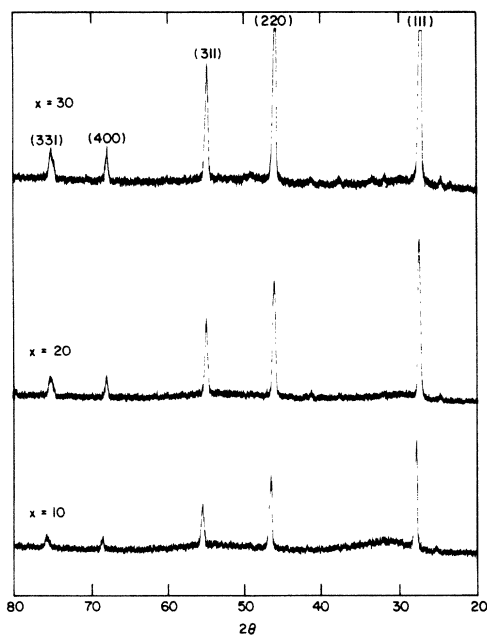


FIG. 3.  $\text{Cu } K\alpha$  diffraction patterns of partially devitrified  $\text{Cu}_x(\text{As}_{0.4}\text{Se}_{0.6})_{100-x}$  alloys with  $x=10, 20,$  and  $30$ .  $(hkl)$  indicates the Miller indices of a sphalerite structure with a lattice parameter of approximately  $5.5 \text{ \AA}$ .

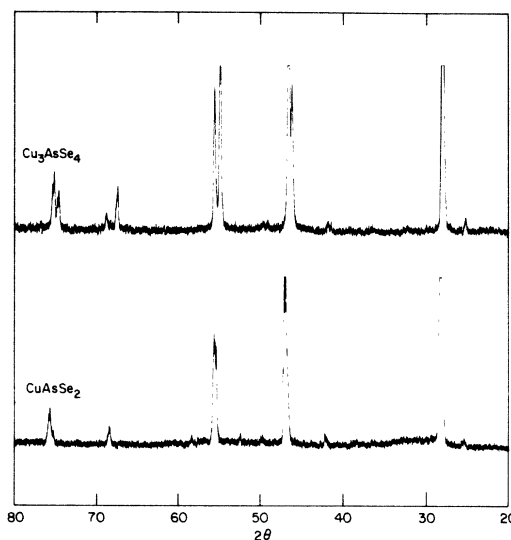


FIG. 4.  $\text{Cu } K\alpha$  x-ray-diffraction patterns of crystalline  $\text{CuAsSe}_2$  and  $\text{Cu}_3\text{AsSe}_4$ .

that the effective cubic  $d$  spacings of these two materials are almost identical, corresponding to an average lattice parameter of approximately  $5.5 \text{ \AA}$ , or a nearest-neighbor distance of  $2.4 \text{ \AA}$ . This latter distance is quite appropriate for covalent bonding, but is much too short for pure ionic bonding.

In their average spacings, both patterns are consistent with that of the crystalline phase found in the devitrified glasses. Since the diffraction pattern from this phase does not show the splittings characteristic of  $\text{Cu}_3\text{AsSe}_4$ , it seems more likely that the phase is  $\text{CuAsSe}_2$ . The extremely small splittings associated with the latter compound could easily become unresolvable through small-crystallite-size broadening or strain broadening of the Bragg peaks. Both phenomena are common in crystals formed from devitrification. The conclusion that the crystalline material is  $\text{CuAsSe}_2$  is reinforced by the melting temperatures observed in the DTA experiments, all of which are equal to or less than  $415^\circ\text{C}$ . The melting temperature of  $\text{CuAsSe}_2$  is  $415^\circ\text{C}$ , while that of  $\text{Cu}_3\text{AsSe}_4$  is  $460^\circ\text{C}$ .

It should be noted that the DTA trace for the sample with  $x=30$  indicates the crystallization and melting of two different crystalline phases. The x-ray diffraction obtained from a sample which had been heated through the second exotherm and then cooled prior to melting was almost identical to that shown in Fig. 3. One possible explanation of this is that both crystalline  $\text{CuAsSe}_2$  and  $\text{Cu}_3\text{AsSe}_4$  form upon heating of this sample. Since the diffraction patterns of these crystalline phases are so similar, the diffraction pattern from a mixture of them would be similar to that shown in Fig. 3.

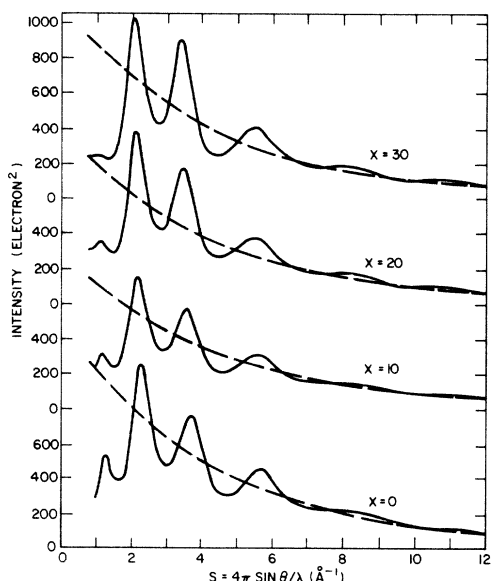


FIG. 5. Scaled, polarization-corrected coherent diffracted intensity as a function of  $s (= 4\pi \sin\theta/\lambda)$  for the  $\text{Cu}_x(\text{As}_{0.4}\text{Se}_{0.6})_{100-x}$  samples. The smooth curves represent the scattering which is independent of atomic configurations, normalized so that the total number of atoms in each sample is unity.

#### IV. X-RAY RADIAL-DISTRIBUTION ANALYSIS

##### A. Experimental procedure and data reduction

X-ray-diffraction patterns from these samples were obtained using zirconium-filtered Mo  $K\alpha$  radiation on a Picker diffractometer, a Nuclear Equipment Corp. solid-state detector, and an ORTEC pulse-height analyzer with window set from 16.4 to 18.5 keV. Therefore, all Compton photons (16.45 keV at  $140^\circ 2\theta$ ) as well as  $K\alpha$  radiation from the Mo source (17.48 keV) were included in the detected intensity data and the  $K\beta$  radiation (19.61 keV) was eliminated. A low-intensity white radiation within the window was also detected and corrected simply by assuming that it contributed a constant to the scattered intensity. It was demonstrated that the results presented here are insensitive to correction, within reasonable bounds.

The intensity data were obtained by scanning continuously at  $\frac{1}{8}^\circ (2\theta)$  per minute and recording the integrated counts for every 100-sec interval. Measurements were made over the angular range  $4^\circ$  to  $145^\circ$ , corresponding to a range in  $s (4\pi \sin\theta/\lambda)$  of 0.62 to 16.85. At the lower angles of observation, the intensity reached a constant value. This constant value was extrapolated to zero angle in the calculation of the Fourier transformation used to determine the radial-distribution function. The

resulting intensities are presented in Fig. 5.

Transformation of the data was performed exactly as described in the work of Betts *et al.*<sup>7</sup> with a value of 0.01 for  $a$  in the arbitrary temperature factor,  $e^{-as^2}$ . Atomic and Compton scattering factors calculated by Benesch<sup>17</sup> were used for Cu, As, and Se. Densities needed for the calculation were measured using a Roller-Smith-Berman density balance. The results, which are presented in Table I, agree fairly well with those reported by Danilov and Myuller<sup>1</sup> and by Savan *et al.*<sup>13</sup>

##### B. Radial-distribution functions and their analyses

Radial-distribution functions (rdf's) of four  $\text{Cu}_x(\text{As}_{0.4}\text{Se}_{0.6})_{100-x}$  samples, with  $x=0, 10, 20,$  and  $30$ , have been obtained and the results are shown in Fig. 6. The first-neighbor peak distances are 2.43, 2.44, 2.45, and 2.46 Å for these samples, respectively. These values are close to the sums of the tetrahedral covalent radii of As-Se (2.32 Å) and Cu-Se (2.49 Å), respectively. The next-neighbor distances are approximately 3.66, 3.73, 3.80, and 3.84 Å, respectively, yielding average bond angles which vary from  $97.98^\circ$  for  $x=0$  to  $102.70^\circ$  for  $x=30$ .

The area under the first peak and the second-peak distance increase steadily with the addition of Cu. The peak height of the first rdf peak changes from  $7 \times 10^3$  electrons/Å<sup>2</sup> for  $x=0$  to  $9 \times 10^3$  electrons/Å<sup>2</sup> for the  $x=10$ . (Here, the independent scattering has been normalized so that the total number of atoms in the sample is unity.) For samples with  $x$  greater than 10, the first-neighbor peak heights remain essentially constant, but the areas increase steadily with increasing  $x$  as a result of broadening of that peak on the high- $r$  side.

Measured areas of the first-neighbor rdf peaks are 2725, 3230, 3635, and 3985 electron<sup>2</sup> for the  $x=0, 10, 20,$  and  $30$  samples, respectively. From these areas, we can attempt to calculate the coordination number of copper. Before doing so, though, we note that these numbers alone indicate that the average coordination number is increasing markedly with increasing  $x$  from the value of 2.4 for pure  $\text{As}_2\text{Se}_3$ . Since As and Se have essentially the same atomic number, while that of Cu is 13% less than their average, the peak areas would decrease slightly with increasing  $x$  if the average

TABLE I. Densities (g/cm<sup>3</sup>) of amorphous Cu-As<sub>2</sub>Se<sub>3</sub> alloys.

As <sub>2</sub> Se <sub>3</sub>	4.544
(As <sub>0.4</sub> Se <sub>0.6</sub> ) <sub>95</sub> Cu <sub>5</sub>	4.733
(As <sub>0.4</sub> Se <sub>0.6</sub> ) <sub>90</sub> Cu <sub>10</sub>	4.894
(As <sub>0.4</sub> Se <sub>0.6</sub> ) <sub>80</sub> Cu <sub>20</sub>	5.206
(As <sub>0.4</sub> Se <sub>0.6</sub> ) <sub>70</sub> Cu <sub>30</sub>	5.577

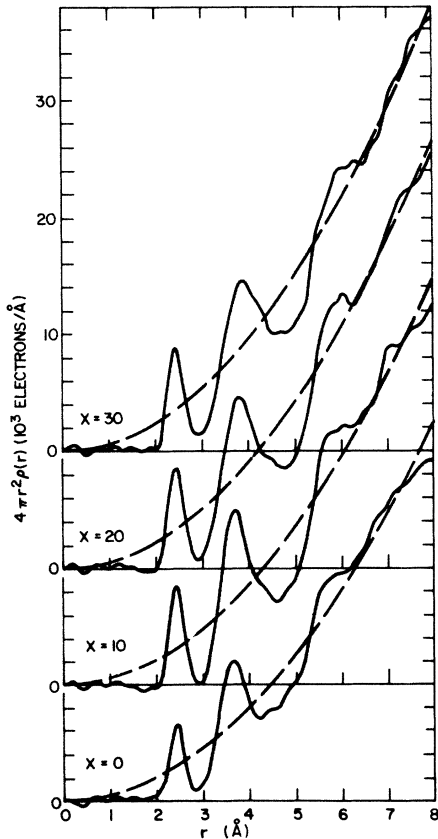


FIG. 6. Calculated radial-distribution functions for the amorphous  $\text{Cu}_x(\text{As}_{0.4}\text{Se}_{0.6})_{100-x}$  alloys, normalized so that the total number of atoms in each sample is unity.

coordination number remained constant. The marked increase of the peak areas with increasing  $x$  indicates directly that the average coordination number is increasing.

In a first effort to determine the Cu coordination, we attempt to fit the area with the random covalent model.<sup>7</sup> In this model, it is assumed that the sample contains threefold coordinated As, twofold coordinated Se, and  $n$ -fold coordinated Cu, with  $n$  to be determined. In the original formulation of this model, it was also assumed that the number of  $A_i$ - $A_j$  pairs  $N_{ij}$  is given by the relation

$$N_{ij} = N_i q_i x_j, \quad (1)$$

where  $N_i$  is the number of  $A_i$  atoms,  $q_i$  is the coordination number of atom  $A_i$ , and  $x_j$  is the atomic fraction of  $A_j$  atoms.

It has been shown by Sayers *et al.*<sup>18</sup> that this formulation cannot be valid because  $N_{ij} \neq N_{ji}$ . This defect can be remedied easily by making  $N_{ij}$  proportional to  $q_j$  as well. Noting that  $N_i = Nx_i$ , where  $N$  is the total number of atoms in the sample, it is readily seen that the resulting expression for  $N_{ij}$  is symmetric in  $i$  and  $j$ , so that  $N_{ij} = N_{ji}$ . Details

of the derivation of the area are given in the Appendix. The resulting equation for the first-neighbor peak area is

$$A = \left( \sum_i x_i q_i Z_i \right)^2 / \sum_i x_i q_i. \quad (2)$$

In this expression, the summation is over the atomic species in the sample,  $x_i$  is the atomic fraction of atom  $i$ , and  $Z_i$  is its effective number of electrons (taken to be the atomic number in this work). For the specific case of the  $\text{Cu}_x(\text{As}_{0.4}\text{Se}_{0.6})_{100-x}$  alloys, this equation becomes

$$A = \frac{[0.4(1-x)3Z_{\text{As}} + 0.6(1-x)2Z_{\text{Se}} + x n Z_{\text{Cu}}]^2}{0.4(1-x)3 + 0.6(1-x)2 + x n}. \quad (3)$$

Figure 7 contains a plot of  $A$  vs  $x$  for various values of  $n$ , as well as the experimental results. The Cu coordination numbers so obtained vary from 8 to 10. Such high coordination numbers for the Cu seem inconsistent with the assumption that all the atoms in the system are bonded in a simple covalent fashion. Hence, we reject this model as a description of the system.

In the neutral-Cu model, it is assumed that the  $\text{As}_2\text{Se}_3$  matrix maintains its coherence, so that each As is bonded to two Se atoms and each Se to three As atoms. The neutral-Cu atoms are con-

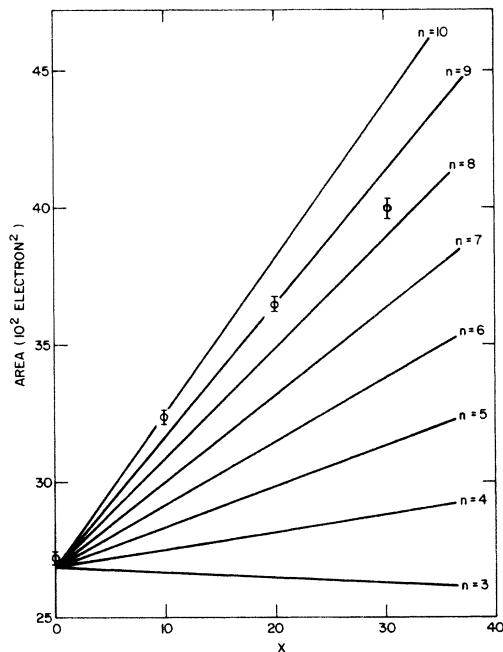


FIG. 7. Area of the first-neighbor rdf peak versus Cu content for amorphous  $\text{Cu}_x(\text{As}_{0.4}\text{Se}_{0.6})_{100-x}$  alloys for various values of the Cu coordination number  $n$ , based on the random covalent model presented here. The experimental areas are noted by  $\Phi$ .

sidered to be interstitial atoms within the resulting  $\text{As}_2\text{Se}_3$  network or metallic clusters. The former model is interesting because it has been used to explain the structure of amorphous Au-Cu-Te alloys.<sup>19</sup> Mössbauer-effect measurements on Te in amorphous  $\text{Te}_{70}\text{Cu}_{25}\text{Au}_5$  suggest that the alloy consists of randomly oriented spiral chains of tellurium with copper and gold atoms randomly distributed between the chains. If this is the case, the same structural model may possibly be applicable to Cu- $\text{As}_2\text{Se}_3$  alloys.

Two calculations incorporating this picture, but making different assumptions about the probability of different types of pairs, yield an average coordination number of approximately 4 for the Cu. Note that in both cases, the average coordinations of As and Se are higher than 3 and 2, respectively, since these atoms are bonded within the  $\text{As}_2\text{Se}_3$  network and also have neutral-Cu neighbors. The importance of this result is that it negates the possibility of the formation of appreciable-sized metallic-Cu clusters with high coordination numbers. Such clusters would have to be sufficiently small so that the large fraction of atoms on the surface would bring the coordination number down from the Cu metallic value of 12. The possibility of neutral-Cu atoms is also negated by the ESCA results described in Sec. V of the paper.

The last model is not a model. Instead, it recognizes the essential ambiguities of interpretation of the first-neighbor peak area of a ternary material in which all types of first-neighbor bonds would involve essentially the same interatomic separations. Hence, it merely states the average coordination number  $\langle q \rangle$ , which is defined as

$$\langle q \rangle = \sum_i x_i q_i \quad (4)$$

for a multicomponent sample, where  $x_i$  and  $q_i$  are the fraction and the coordination number of  $i$ -type atom, respectively. Experimentally,  $\langle q \rangle$  is obtained from the relation

$$\langle q \rangle_{\text{expt}} = A / \left( \sum_i x_i Z_i \right)^2, \quad (5)$$

where  $A$  is the measured rdf peak area in electron units, and  $Z_i$  is the atomic number of the  $i$ -type atom.  $\langle q \rangle_{\text{expt}}$  is particularly meaningful in the Cu-As-Se system because the three  $Z_i$ 's are almost identical.

According to Eq. (5), the observed average coordination number for nearest neighbors is 2.45 for pure  $\text{As}_2\text{Se}_3$ , which agrees very well with the ideal value of 2.40 for a threefold coordinated As and twofold coordinated Se structural picture. However, the most interesting fact is that  $\langle q \rangle$  increases with Cu content to about 3.83 for the 30-at. % Cu sample. This leads us to suspect

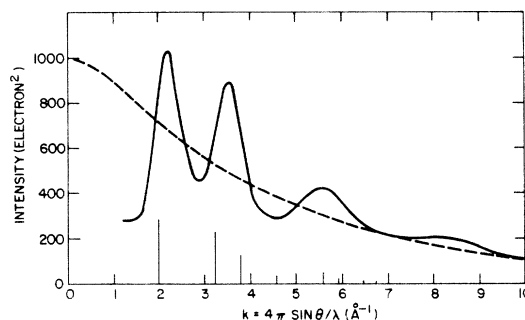


FIG. 8. Scaled, polarization-corrected coherent diffracted intensity as a function of  $s (= 4 \pi \sin \theta / \lambda)$  for glassy  $\text{CuAsSe}_2$ . The smooth curve represents the scattering which is independent of atomic configurations, normalized so that the total number of atoms in the sample is unity.

strongly that the average coordination is approaching the value of 4, associated with the formation of tetrahedral complex, which could be  $\text{CuAsSe}_2$ ,  $\text{Cu}_3\text{AsSe}_4$ , or some other Cu-As-Se alloy. However, from DTA results, which indicate that the major crystalline product of the devitrification process is  $\text{CuAsSe}_2$ , and from ESCA studies, which will be described in the Sec. V, it is shown that  $\text{CuAsSe}_2$  is the most likely complex formed in the Cu- $\text{As}_2\text{Se}_3$  alloys. Hence, it is of considerable interest to study this compound in both crystalline and amorphous forms.

### C. Studies of crystalline and amorphous $\text{CuAsSe}_2$

Some ternary compounds such as  $\text{CuAsSe}_2$ ,<sup>13</sup>  $\text{CdGeP}_2$ , and  $\text{CdGeAs}_2$  (Ref. 20) are known to be tetrahedrally coordinated in their crystalline phases and can be prepared in bulk glassy form. The radial-distribution curves of amorphous  $\text{CdGeP}_2$  and  $\text{CdGeAs}_2$  have been reported.<sup>21</sup> We report here the study of  $\text{CuAsSe}_2$ .

Figure 8 shows the coherently scattered intensity of amorphous  $\text{CuAsSe}_2$ . The powder diffraction peaks of crystalline  $\text{CuAsSe}_2$  are also marked by lines. In the amorphous phase, the first peak falls close to the crystalline (111) peak but with a 0.2 shift to a higher value in  $s$ . The second peak falls close to the average position of the (220) and (311) reflections. A similar shift of the first diffraction peak has also been found in amorphous GaSb and InSb.<sup>22</sup> The radial distribution curves of both crystalline and amorphous  $\text{CuAsSe}_2$  are shown in Fig. 9.

A density problem yields an appreciable uncertainty in the peak area. For crystalline  $\text{CuAsSe}_2$ , the density determined by the Berman method is  $5.28 \pm 0.07 \text{ g/cm}^3$ . The x-ray density obtained by assuming a sphalerite lattice with lattice constant  $5.49 \text{ \AA}$  as determined from x-ray powder diffrac-

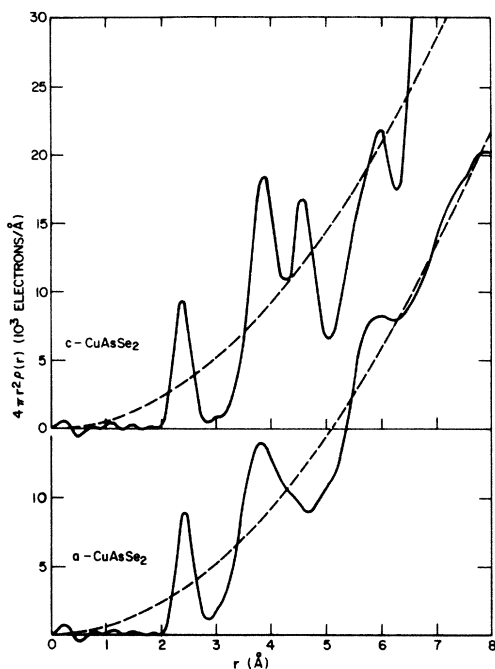


FIG. 9. Calculated radial-distribution functions for crystalline and amorphous  $\text{CuAsSe}_2$ , normalized so that the total number of atoms in each sample is unity.

tion is  $5.950 \text{ g/cm}^3$ . The exact cause of this unusually large discrepancy is not known, but may be an unusually high vacancy concentration.

The nearest-neighbor coordination numbers determined from the rdf of crystalline  $\text{CuAsSe}_2$  are 3.50 and 3.86 when the density is assumed to be 5.28 and  $5.95 \text{ g/cm}^3$ , respectively. Because the tetrahedral coordination has been determined more accurately with the x-ray powder diffraction pattern, we attribute the discrepancy between 3.5 from rdf and 4 of tetrahedral bonding to the density deficit (12.2%) of our crystalline  $\text{CuAsSe}_2$  sample. The first distribution peak is at  $2.41 \text{ \AA}$  and the second peak at  $3.9 \text{ \AA}$ , which corresponds to a bond angle of  $107.82^\circ$ . This value is close to the ideal tetrahedral bond angle of  $109.44^\circ$ . The next nearest coordination number is 13.97, which agrees fairly well with the ideal value of 12.

The rdf of amorphous  $\text{CuAsSe}_2$  shows the average nearest interatomic distance is  $2.44 \text{ \AA}$  and the second-nearest-neighbor peak is at  $3.8 \text{ \AA}$ . Following these relative changes, the average bond angle ( $102.24^\circ$ ) is decreased by  $5.58^\circ$  with respect to that of crystal. The nearest-neighbor coordination number obtained by using the measured density ( $5.276 \text{ g/cm}^3$ ) is 3.49. As with crystalline  $\text{CuAsSe}_2$  we associate the low coordination number with the density deficit rather than any real change of the coordination.

The significant difference between these two rdfs

is seen in the region of the third peak of the crystalline rdf. In crystalline  $\text{CuAsSe}_2$ , the third peak is at  $4.6 \text{ \AA}$ . This peak is about as large as the second peak. In amorphous  $\text{CuAsSe}_2$ , this region corresponds to a minimum of the radial-distribution curve. Similar observations have been made in other tetrahedrally coordinated materials, such as amorphous Si, Ge, and III-V compounds.<sup>23</sup>

Many attempts have been made to explain this general feature of the tetrahedrally coordinated amorphous semiconductors, especially Si and Ge. Three types of structural models have been proposed, including the microcrystallite model, the amorphous-cluster model, and the random-network model.<sup>24</sup> If any of these models is correct, we would expect the same model should be applicable to binary and ternary compounds with sphalerite-related structure as well. Further investigation of the multicomponent compounds would be helpful to the understanding of the common structural feature of the tetrahedrally coordinated amorphous materials. At any rate, the strong similarity of the  $\text{CuAsSe}_2$  rdf to those for the elemental materials, and our knowledge of the crystalline compound shows simple tetrahedral coordination is present in the glassy compound and that the gross features of the amorphous network are similar to those of amorphous Ge, Si, and III-V compounds.

## V. X-RAY PHOTOELECTRON SPECTROSCOPY (ESCA)

### A. Experimental method

Experiments were carried out with a Varian induced-electron-emission spectrometer. The x-ray source can be either aluminum ( $K\alpha$  line at  $1486.6 \text{ eV}$ ) or magnesium ( $K\alpha$  line at  $1253.6 \text{ eV}$ ) anode. The binding energy referred to the Fermi level,  $E_b$ , is obtained from the following relation<sup>25,26</sup>:

$$E_b = E_{x \text{ ray}} - E_{\text{kin}} - \Phi_{\text{sp}}, \quad (6)$$

where  $E_{x \text{ ray}}$  is the energy of the incident x ray,  $E_{\text{kin}}$  is the actual kinetic energy of the photoelectron measured by the spectrometer with respect to the vacuum level, and  $\Phi_{\text{sp}}$  is the work function of the analyzer material.

Each sample was prepared by crushing a chunk to fine powder and rolling the powder on Scotch tape which was attached on the cylindrical aluminum holder. The sample was then put into the spectrometer sample chamber, which was subsequently evacuated to a vacuum of about  $2 \times 10^{-6}$  torr for measurement. Oxygen and carbon contaminations were observed by detecting O 1s and C 2s line intensities, which, however, were found not to affect our results significantly.

When measurements on semiconductors involve this typical procedure, it has been reported that

TABLE II. Chemical shifts of Cu, As, and Se core levels of  $\text{Cu}_3\text{AsSe}_4$ ,  $\text{CuAsSe}_2$ , and  $\text{Cu-As}_2\text{Se}_3$  alloys.

Level	(Ref. energy)	Cryst. $\text{Cu}_3\text{AsSe}_4$	Cryst. $\text{CuAsSe}_2$	Amorph. $\text{CuAsSe}_2$	Amorph. alloys $\text{Cu-As}_2\text{Se}_3$	Partially devitrified $\text{Cu}_{20}(\text{As}_{0.4}\text{Se}_{0.6})_{80}$
Cu $2p_{1/2}$	(951.0) <sup>a</sup>	+0.7	+0.8	+0.9	+1.0	+0.9
Cu $2p_{3/2}$	(931.1) <sup>a</sup>	+0.8	+0.8	+0.9	+0.9	+0.8
As $3s$	(204.1) <sup>b</sup>	+1.7	+1.0	+1.1	+1.2	+0.9
As $3p_{1/2}$	(145.1) <sup>b</sup>	+1.6	+1.2	+1.1	+1.0	+0.9
As $3p_{3/2}$	(140.2) <sup>b</sup>	+1.5	+1.1	+1.0	+1.0	+0.9
As $3d$	(41.2) <sup>b</sup>	+1.6	+1.1	+1.1	+1.1	+1.0
Se $3s$	(229.8) <sup>b</sup>	-0.4	-0.7	-0.7	-0.8	-0.8
Se $3p_{1/2}$	(166.7) <sup>b</sup>	-0.5	-0.6	-0.8	-0.9	-1.0
Se $3p_{3/2}$	(161.0) <sup>b</sup>	-0.5	-0.6	-0.8	-0.8	-1.0
Se $3d$	(55.0) <sup>b</sup>	-0.5	-0.6	-0.8	-0.7	-0.7

<sup>a</sup>From Ref. 27.<sup>b</sup>This work.

$E_b$  can often be shifted owing to the charging effect of the low-conductivity sample. This effect is corrected by using the carbon  $1s$  line as a reference level.

Most of the measurements in this work were made with Mg  $K\alpha$  x-ray and analyzer energy at 100 V, which yielded a full width of the C  $1s$  line at half-maximum intensity about 1.7 to 2.2 eV. The reliability of determining the peak position should be accurate to  $\pm 0.2$  eV without including systematic errors.

### B. Results and discussion

The chemical shift measured with ESCA is the change of binding energy of the atomic core-electron level in a compound, as compared to that in the elemental solid. The cause of the shift is attributed to the redistribution of electric charge that occurs when different chemical bonds are formed in the compound.

As discussed before, a neutral-Cu model has been proposed for the structure of the amorphous  $\text{Au}_5\text{Cu}_{25}\text{Te}_{70}$  alloy. A similar model was also shown to give a reasonable coordination number of Cu in amorphous  $\text{Cu-As}_2\text{Se}_3$  alloys. The validity of this model can be easily tested with ESCA by simply observing the ionization state of Cu in these alloys. ESCA can also be used to study the bonding scheme of  $\text{CuAsSe}_2$ ,  $\text{Cu}_3\text{AsSe}_4$ , as well as  $\text{Cu-As}_2\text{Se}_3$  alloys.

The chemical shifts of core-electron levels of amorphous and partially devitrified  $\text{Cu-As}_2\text{Se}_3$  alloys,  $\text{CuAsSe}_2$ , and  $\text{Cu}_3\text{AsSe}_4$  are given in Table II. The core-electron binding energies of pure Cu are taken from the table of Bearden and Burr,<sup>27</sup> and those of elemental As and Se were measured in this work, which are quite different from the values given by Bearden and Burr. The binding energies of Se core levels measured by us agree very well

with the values reported recently by Shevchik *et al.*<sup>28</sup>

It is apparent that Cu atoms are ionized and a neutral-Cu structural model can be ruled out from our consideration. Comparison of  $2p_{1/2}$  and  $2p_{3/2}$  line spectra of Cu with those of cuprous ( $\text{Cu}_2\text{O}$ ,  $\text{CuCl}$  and  $\text{CuBr}$ ) and cupric ( $\text{CuO}$ ) compounds<sup>9</sup> also leads us to conclude that Cu is singly ionized in  $\text{CuAsSe}_2$ ,  $\text{Cu}_3\text{AsSe}_4$ , and  $\text{Cu-As}_2\text{Se}_3$  alloys. In  $\text{CuO}$  the line splitting of about 1.4 eV of Cu  $2p_{3/2}$  and strong shake up satellites<sup>22,29</sup> were observed, which are presumably due to the spin-spin interaction between the core electrons and the unpaired  $3d$  electrons of the cupric ions. No splitting or satellite was seen in those cuprous compounds and the  $\text{Cu-As-Se}$  system. Study of the magnetic susceptibility in  $\text{As}_2\text{Se}_3$  with Cu additives by Tauc and Menth,<sup>30</sup> which found no paramagnetism, also agrees with our above conclusion.

As compared with the chemical shifts of  $\text{CuAsSe}_2$  and  $\text{Cu}_3\text{AsSe}_4$ , it is interesting to note that all As lines of  $\text{Cu}_3\text{AsSe}_4$  are shifted by about 0.4 eV more than those of  $\text{CuAsSe}_2$ . Although the chemical shift cannot be interpreted quantitatively in a simple manner, we may consider the ionic formula of these two compounds, which can be assigned as  $\text{Cu}^+\text{As}^+\text{Se}_2^{-2}$  and  $\text{Cu}_3^+\text{As}^+\text{Se}_4^{-2}$ . Since As atoms are more ionized in  $\text{Cu}_3\text{AsSe}_4$ , their chemical shifts would be bigger.

It is important to note that amorphous  $\text{CuAsSe}_2$ , amorphous  $\text{Cu-As}_2\text{Se}_3$  alloys, and the partially devitrified  $\text{Cu}_{20}(\text{As}_{0.4}\text{Se}_{0.6})_{80}$  alloy all show chemical shifts which are almost equal to those of crystalline  $\text{CuAsSe}_2$ . This fact becomes important in our attempt to draw conclusions from these studies in Sec. VI.

The valence bands of amorphous  $\text{Cu-As}_2\text{Se}_3$  alloys have also been studied by x-ray photoemission. For  $\text{As}_2\text{Se}_3$ , the valence band extends about 17 eV from the top edge with two distinctive re-

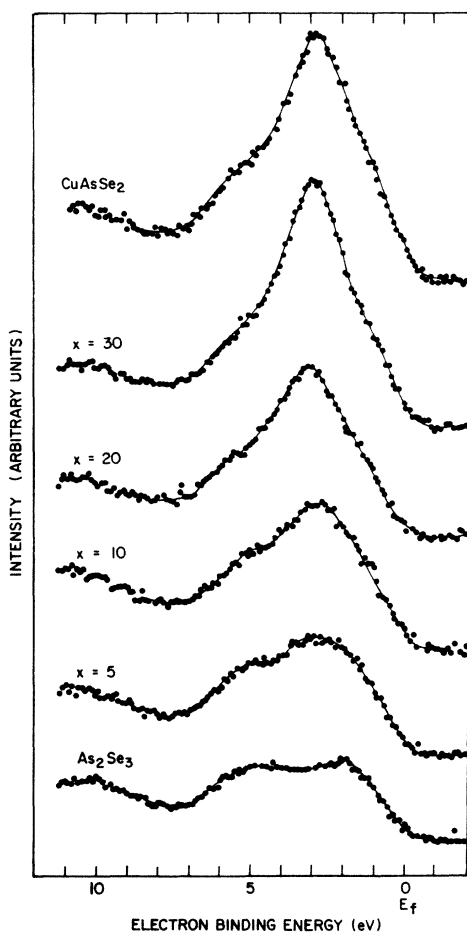


FIG. 10. Valence-band ESCA spectra of amorphous  $\text{As}_2\text{Se}_3$ ,  $\text{CuAsSe}_2$ , and  $\text{Cu}_x(\text{As}_{0.4}\text{Se}_{0.6})_{100-x}$  alloys with  $x=5$ , 10, 20, and 30.

gions.<sup>9</sup> Similar observation has also been reported recently by Fisher.<sup>31</sup> The upper band from 0 to 7 eV is presumably of mainly  $p$  character and the lower band from 8 to 17 eV of  $s$  character made up from  $4p$  and  $4s$  states of As and Se, respectively. The upper band, as shown in Fig. 10, has two peaks at about 2.2 and 5 eV below the Fermi level, which agrees well with the result from uv photoemission by Nielson.<sup>32</sup> The two-peak structure can be understood from the molecular orbitals of this compound as pointed out by Kastner<sup>33</sup> and by Chen.<sup>34</sup> Assuming the  $s$ - $p$  hybridization can be neglected to the first approximation, we may associate the first peak with Se  $4p$  lone pairs and the second peak with As-Se  $\sigma$  bonds.

As Cu is added into  $\text{As}_2\text{Se}_3$ , the major change of the valence band is observed in the upper region as shown in Fig. 10. The figure indicates that a new peak appears at about 3 eV below the Fermi level with the addition of Cu into  $\text{As}_2\text{Se}_3$ . This is presumably due to Cu  $3d$  electrons. If we compare the

valence band of the Cu- $\text{As}_2\text{Se}_3$  system with that of amorphous  $\text{CuAsSe}_2$ , which is also shown in Fig. 10, the resemblance between the valence band of  $\text{CuAsSe}_2$  and that of Cu- $\text{As}_2\text{Se}_3$  alloys with 20–30-at. % Cu is apparent. This agrees (or at least does not conflict) with our structural model proposed in the above, i. e., the formation of a  $\text{CuAsSe}_2$  complex in this alloy system.

## VI. CONCLUSION

At the onset of this work, we sought a structural explanation for the large increase in conductivity and decrease in band gap of Cu- $\text{As}_2\text{Se}_3$  alloys with increasing Cu concentration. The structural work performed here introduced other phenomena to be explained. These are the increase of the nearest-neighbor coordination number and the increase of  $T_g$  with increasing Cu concentration.

It is our belief that these phenomena are reasonably well, but not unambiguously, explained by a model in which the average coordination number goes from 2.4 for pure  $\text{As}_2\text{Se}_3$  to something approaching 4, and in which large portions of the samples have a short-range order similar to that in crystalline  $\text{CuAsSe}_2$ , but on a network similar to that associated with amorphous Ge or Si.

Consider first the decrease in the band gap. Amorphous  $\text{As}_2\text{Se}_3$  has a gap of approximately 1.5 eV, while the alloys with high Cu concentrations have gaps of less than 1 eV. While no gap has, to our knowledge, been published for crystalline or amorphous  $\text{CuAsSe}_2$ , Wernick and Benson<sup>15</sup> indicate that the gap of the former is less than 1 eV. One would expect the gap of the latter to be approximately the same. A superficial explanation for the difference is that  $\text{As}_2\text{Se}_3$  shows strong covalent bonding of the  $8-N$  type, whereas the tetrahedral structure of the compound is due to an average of 4 electrons per atom. The latter type of bonding leads, typically, to gaps of less than 1 eV.

The large increase in the conductivity may be due to the decrease in the gap alone. We note, however, that the increase in coordination could also lead to an increase in the conductivity as a result of the vast increase in the number of, say, hopping paths.

It seems incongruous, at first glance, that the band gap decreases, but  $T_g$  increases, at appreciable Cu concentrations, as the Cu concentration increases. We believe this is due to the different connectivities of the pure  $\text{As}_2\text{Se}_3$  and high-Cu-concentration glasses. Because of its essentially two-dimensional short-range coordination,  $\text{As}_2\text{Se}_3$  may go through a glass transition with less of a disruption of that coordination than the three-dimensionally coordinated glassy  $\text{CuAsSe}_2$ . As a result,  $T_g$  is less simply related to the bond strengths and band gap in  $\text{As}_2\text{Se}_3$  than in  $\text{CuAsSe}_2$ .

The increase in average coordination number is, of course, simply explained by the CuAsSe<sub>2</sub>-component model. We note, however, that the interpretation of radial distributions of ternary systems is necessarily ambiguous. Thus, we feel it necessary to restate the supporting evidence for this picture.

The first is that the first crystallization product from the alloys is apparently CuAsSe<sub>2</sub>. This indicates a relative ease of nucleation of the crystalline compound and lends support to the idea that the atomic arrangement in the amorphous alloys is simply related to that in the crystalline compound.

The second is the similarity of the ESCA core shifts of all the atoms in the alloys to those of crystalline CuAsSe<sub>2</sub>. We note here, though, that a variety of Cu-As-Se compounds might show identical shifts as long as the As<sup>+5</sup> state is not involved.

Finally, there is the similarity between the valence-band structures of the high-Cu-concentration alloys and that of glassy CuAsSe<sub>2</sub>.

This evidence, taken in its entirety, does not constitute a proof that there is a change in structure to something like that in CuAsSe<sub>2</sub>. Nevertheless, it is strongly inferential, and about the best we can do with such a complex system and the techniques available to us. There is no doubt, however, that the average coordination number increases markedly and that, consequently, the simple, strongly covalent, 8-N bonding of pure As<sub>2</sub>Se<sub>3</sub> is breaking down with appreciable Cu concentrations.

#### ACKNOWLEDGMENTS

We are indebted to Marta de Rojas of Stanford University's Center for Materials Research for her assistance with the x-ray diffraction experiments. Thanks are due to Varian Associates for the use of their IEE spectrometer and Dr. W. G. Proctor and Dr. J. Smith for their assistance in making the ESCA measurements. Conversations of K. L. with Dr. I. Lindau have also been helpful.

#### APPENDIX: NEW RANDOM COVALENT MODEL

As indicated in the text, Sayers *et al.*<sup>18</sup> have shown that the random covalent model (RCM) of Betts *et al.*<sup>7</sup> is unsatisfactory. In that model, the number of A<sub>i</sub>-A<sub>j</sub> pairs N<sub>ij</sub> is not, in general, equal to N<sub>ji</sub>.

In this appendix a new RCM is presented in which that defect is corrected.

Consider an alloy system consisting of *n* atomic species A<sub>*i*</sub>, *i* = 1, ..., *n*. Let *x<sub>i</sub>* be the atomic fraction of each species, so that

$$\sum_i x_i = 1. \quad (\text{A1})$$

If *q<sub>i</sub>* is the coordination number of each species, the total number of near-neighbor bonds per atom in the system is

$$Q = \frac{1}{2} \sum_i x_i q_i. \quad (\text{A2})$$

We now proceed to calculate the number of near-neighbor pairs per atom in the sample, of type A<sub>*i*</sub>-A<sub>*j*</sub>, denoted N<sub>ij</sub>. Consider, first, the case *i* ≠ *j*. That number is proportional to *x<sub>i</sub>q<sub>i</sub>*. For a random alloy, we also assume it is proportional to *x<sub>j</sub>q<sub>j</sub>*. Then,

$$N_{ij} = C x_i x_j q_i q_j = N_{ji}, \quad (\text{A3})$$

where *C* is a constant to be determined. For *i* = *j*, a factor of 2 must be introduced because each pair would be counted twice otherwise. Hence,

$$N_{ii} = C x_i^2 q_i^2 / 2. \quad (\text{A4})$$

The total number of pairs is then

$$Q = (C/2) \sum_i x_i^2 q_i^2 + (C/2) \sum_i \sum_j' x_i x_j q_i q_j, \quad (\text{A5})$$

In Eq. (A5), the prime on the summation sign indicates that terms with *i* = *j* are excluded and the factor of 1/2 on the second term of the right-hand side is included to take account of the double counting associated with the double summation. Eq. (A5) can be rewritten as

$$\begin{aligned} Q &= (C/2) \sum_i \sum_j x_i x_j q_i q_j \\ &= (C/2) \left( \sum_i x_i q_i \right)^2 \\ &= 2CQ^2, \end{aligned}$$

so that

$$C = 1/2Q. \quad (\text{A6})$$

The area *A* of an x-ray-diffraction rdf first-neighbor peak is obtained by weighting each pair by the product of the effective number of electrons, *Z<sub>i</sub>*, associated with the atoms in the pair, summing over pairs, and multiplying by 2. Hence,

$$\begin{aligned} A &= (1/2Q) \left( \sum_i x_i q_i Z_i \right)^2 \\ &= \left( \sum_i x_i q_i Z_i \right)^2 / \sum_i x_i q_i. \end{aligned} \quad (\text{A7})$$

\*Research supported in part by the Advanced Research Projects Agency of the Department of Defense and monitored by the U. S. Army Research Office—Durham,

under Contract No. DAHC04-70-C-0044 and Grant No. DA-AR0-D-31-124-72-G151, and by the National Science Foundation through the Center for Materials Re-

- search at Stanford University.
- †Present address: Xerox Webster Research Center, Xerox Square, Rochester, New York, 14644.
- <sup>1</sup>A. V. Danilov and R. L. Myuller, *Zh. Prikl. Khim.* **35**, 2012 (1962).
  - <sup>2</sup>A. V. Danilov and M. El. Mosli, *Fiz. Tverd. Tela* **5**, 2015 (1963) [*Sov. Phys.-Solid State* **5**, 1472 (1963)].
  - <sup>3</sup>J. T. Edmond, *J. Non-Cryst. Solids* **1**, 39 (1968).
  - <sup>4</sup>B. T. Kolumiets, Yu. V. Rukhlyadev, and V. P. Shilo, *J. Non-Cryst. Solids* **5**, 402 (1971).
  - <sup>5</sup>A. E. Owen, *Glass Ind.* **48**, 637, 695 (1967).
  - <sup>6</sup>N. F. Mott, *Adv. Phys.* **16**, 49 (1967).
  - <sup>7</sup>F. Betts, A. Bienenstock, and S. R. Ovshinsky, *J. Non-Cryst. Solids* **4**, 554 (1970).
  - <sup>8</sup>A. L. Renninger and B. L. Averbach, *Phys. B* **8**, 1507 (1973).
  - <sup>9</sup>K. S. Liang, Ph.D. thesis (Stanford University, 1973) (unpublished).
  - <sup>10</sup>R. Andreichin, *J. Non-Cryst. Solids* **4**, 73 (1970).
  - <sup>11</sup>J. Tauc and A. Menth, *J. Non-Cryst. Solids* **8/10**, 569 (1972).
  - <sup>12</sup>N. F. Mott and E. A. Davis, *Electronic Process in Non-crystalline Materials* (Oxford U. P., London, 1971), p. 340.
  - <sup>13</sup>Ya. Savan, I. I. Kozhina, and Z. U. Borisova, *Vestn. Lening. Univ. Ser. Fiz. Khim.* **22**, No. 10, 141 (1967).
  - <sup>14</sup>Y. Asahara and T. Izumitani, *J. Non-Cryst. Solids* **11**, 97 (1972).
  - <sup>15</sup>J. H. Wernick and K. E. Benson, *J. Phys. Chem. Solids* **3**, 157 (1967).
  - <sup>16</sup>G. Busch and F. Hulliger, *Helv. Phys. Acta* **33**, 657 (1960).
  - <sup>17</sup>R. Benesch, M.S. thesis (University of Alberta, 1972) (unpublished).
  - <sup>18</sup>D. E. Sayers, F. W. Lytle, and E. A. Stern, in *Proceedings of the Fifth International Conference on Amorphous and Liquid Semiconductors, Garmish-Partenkirchen, 1973* (to be published in *J. Non-Cryst. Solids*).
  - <sup>19</sup>C. C. Tsuei and E. Kankeleit, *Phys. Rev.* **162**, 312 (1967).
  - <sup>20</sup>A. A. Vaipolin, N. A. Goriunova, E. O. Osmanov, and Yu. V. Rud, *Dokl. Akad. Nauk SSSR Ser. Phys. Chem.* **160**, 633 (1965) [*Proc. Acad. Sci. USSR Phys. Chem. Sect.* **160**, 74 (1965)].
  - <sup>21</sup>R. Grigorovici, R. Manaila, and A. A. Vaipolin, *Acta Crystallogr. B* **24**, 535 (1968).
  - <sup>22</sup>T. Novakov and R. Prins, *Solid State Commun.* **9**, 1975 (1971).
  - <sup>23</sup>N. J. Shevchik, Harvard University Technical Reports No. HP-29 and No. ARPA-44 (unpublished).
  - <sup>24</sup>D. Turnbull and D. E. Polk, *J. Non-Cryst. Solids* **8/10**, 19 (1972).
  - <sup>25</sup>K. Siegbahn *et al.*, Air Force Materials Laboratory, Ohio, Technical Report No. AFML-TR-68-189, 1968 (unpublished).
  - <sup>26</sup>D. W. Langer and C. J. Vesely, *Phys. Rev. B* **2**, 4885 (1970).
  - <sup>27</sup>J. A. Bearden and A. F. Burr, *Rev. Mod. Phys.* **39**, 125 (1967).
  - <sup>28</sup>N. J. Shevchik, M. Cardona, and J. Tejada, *Phys. Rev. B* **8**, 2833 (1973).
  - <sup>29</sup>T. Robert, M. Bartel, and G. Offergeld, *Surf. Sci.* **33**, 123 (1972).
  - <sup>30</sup>J. Tauc and A. Menth, *J. Non-Cryst. Solids*, **8/10**, 569 (1972).
  - <sup>31</sup>G. B. Fisher, *Bull. Am. Phys. Soc.* **18**, 1589 (1973).
  - <sup>32</sup>P. Nielson, *Bull. Am. Phys. Soc.* **17**, 113 (1972).
  - <sup>33</sup>M. Kastner, *Phys. Rev. Lett.* **28**, 355 (1972).
  - <sup>34</sup>I. Chen, *Phys. Rev. B* **8**, 1440 (1973).